Dentomaxillofacial Radiology (2018) 47, 20170345

birpublications.org/dmfr

RESEARCH ARTICLE

Evaluation of natural mandibular shape asymmetry: an approach by using elliptical Fourier analysis

[1]Tania C Niño-Sandoval, [2]Carlos F Morantes Ariza, [3]Clementina Infante-Contreras and [4]Belmiro CE Vasconcelos

[1]Department of Oral and Maxillofacial Surgery, University of Pernambuco, Camaragibe, Brazil; [2]Department of Biology, National University of Colombia, Bogotá, Colombia; [3]Department of Oral Health, Growth and Development research line, National University of Colombia, Genetics Institute, Bogotá, Colombia; [4]Department of Oral and Maxillofacial Surgery, University of Pernambuco, Camaragibe, Brazil

Objectives: The purpose of this study was to demonstrate that asymmetry is a natural occurring phenomenon in the mandibular shape by using elliptical Fourier analysis.
Methods: 164 digital orthopantomographs from Colombian patients of both sexes aged 18 to 25 years were collected. Curves from left and right hemimandible were digitized. An elliptical Fourier analysis was performed with 20 harmonics. In the general sexual dimorphism a principal component analysis (PCA) and a hotelling T^2 from the multivariate warp space were employed. Exploratory analysis of general asymmetry and sexual dimorphism by side was made with a Procrustes Fit. A non-parametric multivariate analysis of variance (MANOVA) was applied to assess differentiation of skeletal classes of each hemimandible, and a Procrustes analysis of variance (ANOVA) was applied to search any relation between skeletal class and side in both sexes.
Results: Significant values were found in general asymmetry, general sexual dimorphism, in dimorphism by side ($p < 0.0001$), asymmetry by sex, and differences between Class I, II, and III ($p < 0.005$). However, a relation of skeletal classes and side was not found.
Conclusions: The mandibular asymmetry by shape is present in all patients and should not be articulated exclusively to pathological processes, therefore, along with sexual dimorphism and differences between skeletal classes must be taken into account for improving mandibular prediction systems.
Dentomaxillofacial Radiology (2018) **47**, 20170345. doi: 10.1259/dmfr.20170345

Cite this article as: Niño-Sandoval TC, Morantes Ariza CF, Infante-Contreras C, Vasconcelos BCE. Evaluation of natural mandibular shape asymmetry: an approach by using elliptical Fourier analysis. *Dentomaxillofac Radiol* 2018; **47**: 20170345.

Keywords: mandibular asymmetry; sexual dimorphism; elliptical fourier analysis; hemimandibular shape

Introduction

Mandibular reconstruction is a necessary process after a mandibulectomy to help with the recovery of the quality of life of the patient at functional and aesthetic level. The processes involved in reconstructive surgery must be related to results that resemble a mandibular morphological reality. Currently, several customized methods are used but they represent a high cost and unfortunately do not report meticulously the inclusion of anthropometric characteristics that define the mandibular morphology, such as differences between males and females, classes or mandibular asymmetry.

Asymmetry is a characteristic attributed to congenital or acquired pathological processes. Historically, it has been associated with an active region of growth that surpasses its counterpart.[1] However, although the right and left sides of the mandibular bone have very similar processes in their growth and development, there are

Correspondence to: Mrs Tania C Niño-Sandoval, E-mail: kotc2578@gmail.com
Received 10 September 2017; revised 16 March 2018; accepted 19 March 2018

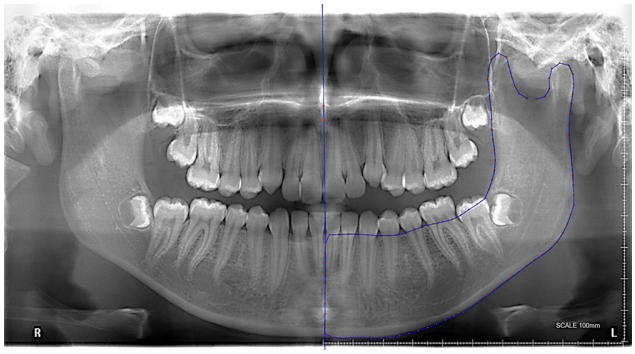

Figure 1 Curve of left hemimandible.

some external and internal factors which could influence the shape of the mandibular bone.[2] From this concept, it can be inferred that asymmetry could be present naturally in all individuals in different levels without necessarily being linked with abnormality factors;[3] however this premise has not been well studied.

The development of new proposals for mandibular prediction and reconstruction is a growing field. In order to carry out a system accessible to the low-income Latin American population, that also has a proper mandibular morphology to the actual craniofacial conformation of the patient, it is proposed to employ two-dimensional elements such as analysis in panoramic radiographs to be extrapolated in a three-dimensional view. Approaches in prediction in other types of radiographs have been made in terms of size and position;[1,4–7] however from a posteroanterior view according to a previous study,[8] a discrepancy could be observed between the left and right side prediction coefficients, with an important influence of the mandibular shape.

Because the use of lines and angles are limiting when analyzing the mandibular shape, defined as the characteristic that remains after filtering size and position attributes, the inclusion of elements of geometric morphometrics such as the analysis of contours can give a more detailed morphological description of this property due to its capability for synthesizing the multivariate nature of morphological variation into simpler descriptors.[9] To obtain a quantification of a contour drawn in a panoramic radiograph, an elliptical Fourier analysis (EFA) is used. When a contour is traced on a surface or edge, it is composed of an arbitrary number of landmarks that defines its outline. However, this figure is projected on a cartesian system not as a function, but as a relation. That is, a single X coordinate may have two or more values in Y axis. This situation limits the

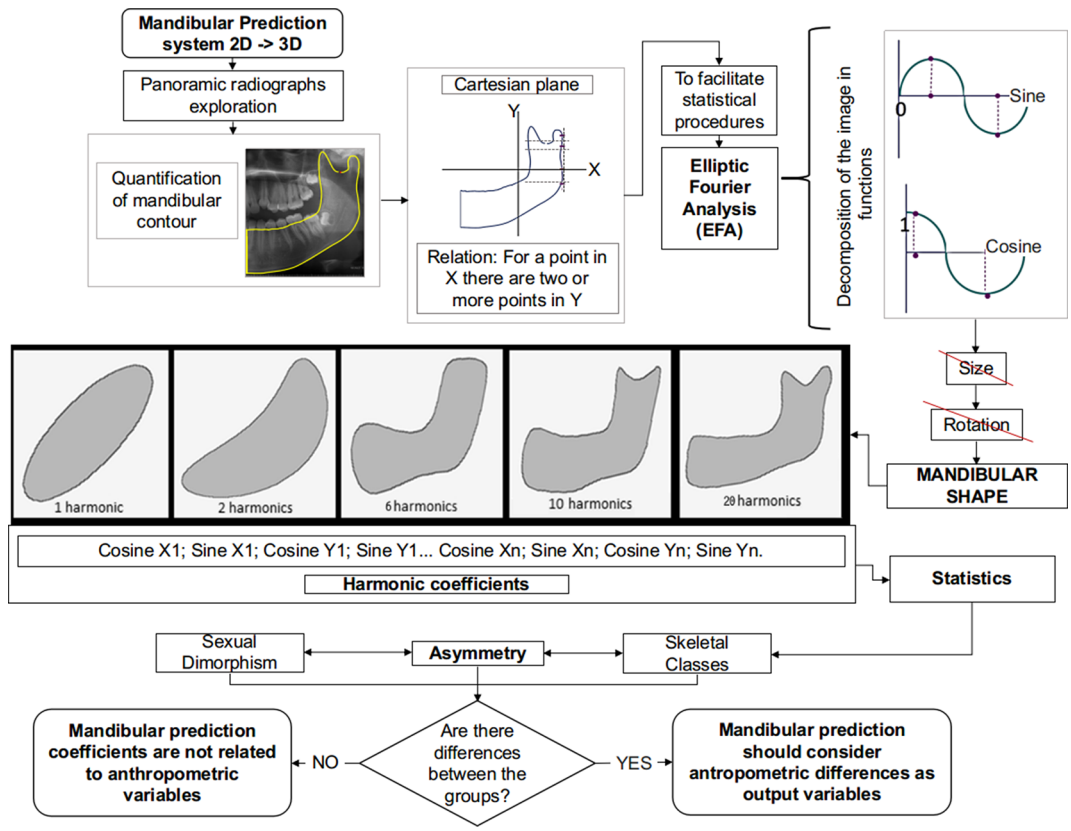

Figure 2 Principal EFA deformations.

Table 1 Multivariate normality test and a homogeneity of variances test

Multivariate normality test (Mardia)				
Multivariate	*Coefficient*	*Statistic*	*df*	*p (normal)*
Skewness	30.3	1657	364	1.067 E-163
Skewness, small sample corrected		1674	364	1.13 E-166
Kurtosis	196.3	13.97		0
Doornik and hansed omnibus				
Ep:		201.5		
p (normal)		5.302E-30		
Box's M: 157.43	Monte Carlo *p* (equal): 0.01		*p* (equal): 1.2588E-06	

performance of statistical analyses traditionally used to assess mandibular asymmetry. For this reason, EFA is applied to decompose these relations in functions of sines and cosines.[9–11]

To perform this, several ellipses are traced around the structure. The first ellipse represents the main angular characteristics of the structure, and each ellipse depends hierarchically, based on the amount of information provided by its trajectory, on the previous execution and is composed of functions of sines and cosines. These sets of functions are called harmonics. The arrangement continues successively until there are sufficient functions to accurately reproduce the topology of the structure and consecutive ellipses add no significant variation when compared to the previous ones.[9] This gives numerical values that can be used for statistical analysis and prediction processes, the union of all these data will reconstruct an image of the mandible and this information is useful for two-dimensional models that can be extrapolated to create three-dimensional models.

As a first step to achieve the model of two-dimensional to three-dimensional prediction, it is important to know if it is necessary to make the mandibular prediction of the left side separately from the right side or as a single component, that is, to observe if natural asymmetry is a factor linked to the mandibular shape and is not a size feature, as reported in several studies.[5,7,12,13] Also other factors such as sexual dimorphism and skeletal classes linked to asymmetry could influence the mandibular shape. The foregoing analysis could confirm one hypothesis established in the mentioned study about that the asymmetry affects the general mandibular prediction. Besides, the results of this approach can be a starting point to establish the output variables and the distribution groups for creating more precise prediction systems.

Methods and materials

Sample

The design of the current study was retrospective with a non-probability convenience sampling; it consisted of digital orthopantomographs from 164 patients of the Faculty of Dentistry of the National University of Colombia, aged 18–25. For each radiography, data of lateral cephalograms including the ANB angle to establish skeletal classifications was available, therefore the information of 66 females (30 Class I, 17 Class II, 19 Class III) and 98 males (40 Class I, 22 Class II, and 36 Class III) was used.

To obtain the radiographic images, a single X-ray unit Veraviewepocs of J Morita model X550, Type EX-1, was used. An AF Automatic Positioning light beam sensor was used for proper patient alignment, decreasing positioning errors. A shadow reduction panoramic projection and an orthoradial panoramic projection were employed, reducing obstructing shadows and overlapping structures respectively. The application software for image processing was the I-Dixel of J. Morita Mfg. Corp, achieving 100% (1:1) images, allowing to incorporate a digital X-ray ruler, to set each radiograph scale.

The selection criteria included a complete permanent dentition with third molars in similar position. Patients with previous orthognathic or orthodontic treatment, orthopedic and/or aesthetic surgery, severe parafunctional habits and congenital or acquired malformations were excluded; this information is available in the database of the Master of Dentistry of the National University of Colombia, described in Niño-Sandoval et al.[14]

All participants in this study signed an informed consent considering the principles stated in the Declaration of Helsinki "Ethical Principles for Medical Research Involving Human Subjects". Also, ethics considerations were based according to Law 84 of the 1989 Colombian constitution in its resolution 008,430 which establishes the scientific, technical, and administrative norms for the investigation in health.[15] Additionally, this study was approved by the ethics committee of the Faculty of Odontology of the National University of Colombia, under registration number CIE-0009–10.

TPSDig2 software (Rohlf, F. J. 2005. TpsDig, digitize landmarks and outlines, v. 2.05. Department of Ecology and Evolution, State University of New York, Stony Brook, NY) was employed to digitize the curves in each hemimandible. The midpoint of the intersection of the anterior nasal spine with the palatal process of the maxilla (ENA) and the intersection of the lowest point of the anterior nasal spine with the upper alveolar border of the maxilla (ENA') were located. A reference straight line which passes through these landmarks was traced in all the radiography in order to establish the anterior spinal plane or Sagittal Plane (Plane S); this plane defines the limit of the midline of each hemimandible, as described in Jiménez et al.[16]

The contour was drawn starting in the deepest zone of the mandibular sigmoid notch. At the end of the graphing process, the curve was resampled by length in 100 equidistant points to define the mandibular bone with high fidelity (Figure 1). Left side was drawn first

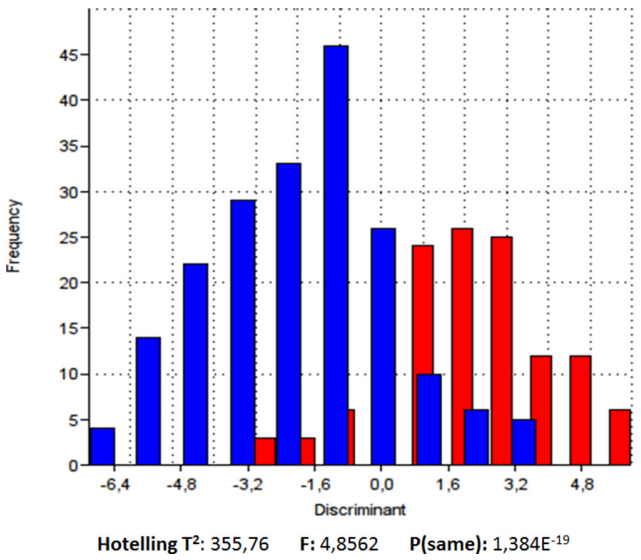

Figure 3 Hotelling T^2 for sexual dimorfism.

and then, the image was rotated to draw the right side, taking into account the Plane S.

Elliptical fourier analysis

PAST software (Hammer, Ø, Harper, DAT, Ryan, PD. 2013. PAST: Paleontological Statistics software package for education and data analysis, v. 2.17c. Paleontological Museum, University of Oslo, Sars gate1, 0562 Oslo, Norway.) was employed to generate the elliptical Fourier function (Figure 2). First, a mathematical relation of the outlines was transformed in functions. Visual observation leads to choose until the first 20 elliptical Fourier harmonics. As these were calculated invariant to the start point, rotation, and size (Figure 2), possible positioning errors that could be remaining after taking the radiographs can be controlled, because at this point mandibular shape property has not relation with any size feature such as magnification. With this data transformation, sexual dimorphism was determined to distribute the analysis groups.

For this task, a principal component analysis (PCA) was performed, in this, the contribution of each harmonic to the total variance of the sample is observed. A Box's M test was applied, in which homoscedasticity was found; hence, a Hotelling T^2 from the multivariate mean vector was applied. This test creates a synthetic variable by means of variance/covariance matrix and projects the individuals over this variable. Finally, a two-group multivariate permutation (i = 1999) analysis was used to randomize the sample while the discriminant function was applied.

An exploratory analysis was performed on the landmarks reconstruction from the elliptical Fourier harmonics, to study the asymmetry and contemplate sexual dimorphism by side to characterize entirely the mandibular morphology. To achieve this, the EFAwin software (Isaev, M. 2010. V. 2.1. Department of Ecology and Evolution, State University of New York, Stony Brook, NY) was used to obtain a mathematical approximation of the curve. Then, with the reconstructions data, MorphoJ software (Klingenberg, C P. 2011. MorphoJ: an integrated software package for geometric morphometrics. V. 1.06d. Manchester, UK) was used to perform a Procrustes Fit (GPA) aligned by principal axes. This superimposition algorithm removes size by normalizing every individual within the sample to the same size. It also removes position noise information by rotating and aligning all individuals to fixed principal axes.

Once this has been done, GPA estimates the hypothetical configuration that is closer to every subject in the sample. This is achieved by least square error residuals reduction through multiple iterations of the fitting process. A covariance matrix that includes the left and right side, and both sexes was generated in the reconstructed file. After that, a discriminant function was applied, including all pairs of groups and an additional test with 1000 permutations was performed. Permutations are used to find robust differences between the projected groups because it operates under the assumptions that even when random individuals are removed from the sample, the remaining subjects can account for the observed difference. Thus, a high number of permutations will reduce variations due to atypical observations within the sample.

Considering skeletal classes of each hemimandible, inferential, and exploratory analysis of its shapes were

Table 2 Discriminant function of asymmetry and sexual dimorphism by side

	General asymmetry	*Sexual dimorphism left side*	*Sexual dimorphism right side*	*Feminine asymmetry*	*Masculine asymmetry*
Difference between means:					
Procrustes distance	0,01686047	0,03008796	0,02587101	0,01475814	0,01925929
Mahalanobis distance	1,6847	3,3115	3,2773	3,3081	2,2181
T^2	232,7253	432,5026	423,6089	361,1342	241,0879
p-Value (parametric)	<0.0001	<0.0001	<0.0001	0,0284	0,0040
p-values for permutation tests (1000 permutation runs):					
Procrustes distance	0,0168	0,0160	0,0470	0,3500	0,1150
T^2	<0.0001	<0.0001	<0.0001	0,0260	0,0040

The permutation test using the T^2 statistic is equivalent to a test using Mahalanobis distance.

Table 3 Non-parametric MANOVA

	Feminine Class I	*Feminine Class II*	*Feminine Class III*	*Masculine Class I*	*Masculine Class II*	*Masculine Class III*
Feminine Class I		0.0015	0.0015	1	0.0015	0.0015
Feminine Class II	0.0015		0.0015	0.0015	1	0.0015
Feminine Class III	0.0015	0.0015		0.0015	0.0015	1
Masculine Class I	1	0.0015	0.0015		0.0015	0.0015
Masculine Class II	0.0015	1	0.0015	0.0015		0.0015
Masculine Class III	0.0015	0.0015	1	0.0015	0.0015	

made to understand and locate graphically the differences between them. First, a multivariate normality test and homogeneity of variances test were made as shown in Table 1 (H_0: Normality/homoscedasticity). As data do not follow a parametric distribution, a Non-parametric MANOVA was used with the values of the coefficients of the harmonics (sine and cosine functions).

In this analysis, an Euclidean distance was used. However, as this distance does not consider the loss of degrees of freedom, then the *p* value was adjusted to a Bonferroni corrected value that tightens the hypothesis test to reduce the risk of Type I error. In addition, Procrustes ANOVA was applied to know the variation at the level of conformation in terms of class and side and to analyze if one variable explains the other in males and females.

To understand in a practical way the distribution by sex and class, two principal components plots from the EFA of the mean shapes were constructed, additionally to characterize the morphological differences of the mean shapes of each group (that includes side, sex, and class) with the general consensus, a heat map by expansion factors with 20 grid lines, which explains in colors the amount of relative deformations that suffers the morphology of the hemimandible, was shown.

Results

Figure 3 shows the sexual dimorphism with PCA by Hotelling T^2. The first three components show variance percentage values of 28,383, 24,91, and 15,842 (total explained variance = 69.14%). The difference between males' group (blue and females' group (red) is statistically significant ($p < 0.0001$).

Table 2 shows significant values ($p < 0.0001$) that can be observed for the study of general asymmetry, concluding that both sides differ in the entire studied sample. Also, significant values ($p < 0.0001$) that can be observed between males and females on each side were being consistent with the previous results regarding sexual dimorphism. For the asymmetry study by sex, significant values ($p < 0.005$) were obtained for both female and male population, concluding that there is asymmetry in the conformations of each hemimandible in both sexes.

Table 3 shows significant differences between the skeletal classes in both sexes. However, sexual dimorphism of the same skeletal classes, in this case is not significant.

Tables 4 and 5 confirm the skeletal class differences and asymmetry of the shape both in masculine and feminine samples, however there is not a relationship between side and class.

Figures 4 and 5 show the principal components plots from the EFA from the mean shapes by side and class respectively. The first component has 59,237% of contribution to the variance, the second of 29,191%; therefore, the graphs explain 88.42% of the contribution. The nomenclature of the groups is as follows: the first character could be 1 that indicates the left side, or could be 0 for the right side; the second character could be F for the feminine sample, or M for the masculine sample; the last character could be 1, 2, or 3 for skeletal pattern Class I, II, and III respectively. It can be seen in Figure 4a, general separation between sides confirming the asymmetry. However, there is an overlapping of left side feminine Class II and Class I (upper figure) in the right-side data, indicating that despite the differences shapes are similar.

On the other hand, Figure 5 shows the differences between classes; Class III (upper figure) is well defined by its shape by sex and side. In general terms, it can be seen as the separation between Class I (middle figure) and Class II (lower figure); however there is an

Table 4 Shape, Procrustes ANOVA in masculine sample

Effect	*SS*	*MS*	*df*	*F*	*p*
Class	0,01873360	0,0000477898	392	3,20	<0.0001
Side	0,01811619	0,0000924296	196	6,18	<0.0001
Class*Side	0,00586220	0,0000149546	392	0,34	1,0000
Residual	1,65736072	0,0000445049	3,7240		

ANOVA, analysis of variance.

Table 5 Shape, Procrustes ANOVA in feminine sample

Effect	*SS*	*MS*	*df*	*F*	*p*
Class	0,01936094	0,0000493902	392	14,34	<0.0001
Side	0,00716885	0,0000365758	196	10,62	<0.0001
Class*Side	0,00135028	0,0000034446	392	0,09	1,0000
Residual	0,91419829	0,0000370181	2,4696		

ANOVA, analysis of variance.

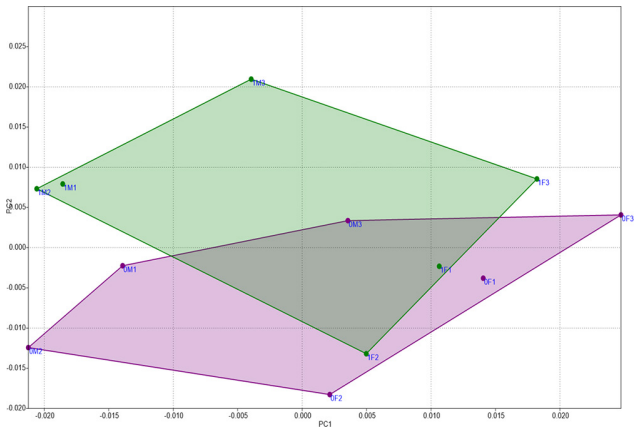

Figure 4 Principal components from EFA by side. EFA, elliptical Fourier analysis.

overlapping in Class I in the masculine right side. Moreover, Figures 6 and 7 show the heat maps from the consensus shape in each group, in females and males respectively. The red color and those that have tendency to this color indicate the sites of greater variation of the shape of each subgroup in comparison with the general consensus. The blue sites and those that are closer to this indicate the mandibular morphological areas where there is not any major variation.

In Figure 6, it can been seen that in left side Class I, the main differences occur in the central part of the midline with a superior and anterior direction; besides, there is an important variation arising from the central part of the mandibular ramus until the sigmoid notch and there is a relevant difference in the coronoid process with a superior and posterior direction (Figure 6a). For the left side Class II, the difference is originated in the base of the coronoid process and descends in the posterior zone of the gonial angle (Figure 6b).

In left side Class III and in right side Class I, the main difference occurs in the lower zone of the midline in a superior and anterior direction (Figure 6c,d). Right side Class II shows differences from the center of the base of the mandibular ramus and is directed lower and

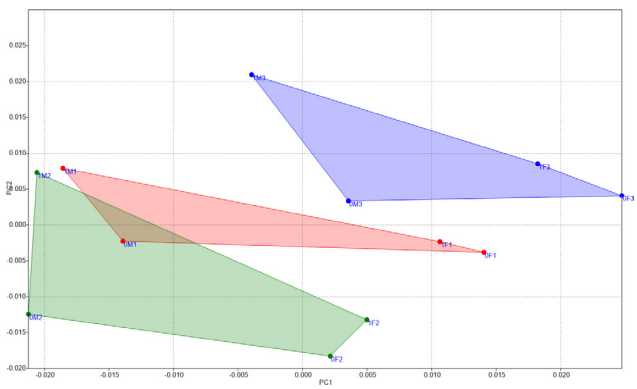

Figure 5 Principal components from EFA by class. EFA, elliptical Fourier analysis.

posteriorly until the posterior zone of the gonial angle (Figure 6c,d). Finally, right side Class III shows differences in the superior part of the midline directed anteriorly and in a slight portion of the superior anterior zone of the condyle directed downwards (Figure 6f).

In males, left side Class I (Figure 7a) shows the main difference from the alveolar ridge in an ascending direction and in a portion of the coronoid process such as left side Class II have a posterior and superior direction (Figure 7b). For left side Class III, the differences occur in the alveolar ridge in ascending direction, in the superior portion of the midline in anterior direction, in the most anterior portion of the mandibular lower border with a posterior inferior direction, and a slight posterior region of the head of the condyle directed backwards (Figure 7c).

For the right sides, in Class I, the main difference occurs in the condylar neck with a posterior direction (Figure 7d). In Class II, most of the mandibular bone had important differences except in the midline, in the mandibular body next to the lower border, the direction of variation is downwards but from the middle region of the mandibular body the variation occurs upwards; from the base of the mandibular ramus there is a variation in posterior and inferior direction towards the gonial angle.

Additionally, in the base of the mandibular ramus there are another three variation: the first one has an anterior superior direction that reaches the coronoid process, the second one is upwards until the sigmoid notch and the last one is directed posterior superiorly for reaching the condylar neck (Figure 7e), finally, Class III show differences in the base of the coronoid process with a superior anterior direction and also in the superior part of the condyle with a upward direction (Figure 7f).

Discussion

The importance of the mandibular shape characterization is reflected in the creation of more precise mandibular prediction systems to achieve a more accurate modeling. These can be used in several mandibular bony defects that result from pathological processes. Algorithms like the mirroring algorithm are useful tools to reconstruct virtually these defects by reproducing the healthy side in the affected side. However, when all the hemimandible is reproduced shows a symmetrical mandible that is not natural and not adaptable to the patient's reality. Khalifa et al aware of this situation applied mirror algorithms in specific parts without affecting the general mandibular shape.[17]

However, this situation is complicated when the mandibular defects affect almost the entire hemimandibular segment. The results of this work helps to improve aspects considered in previous researches about mandibular prediction,[8] and it can be established that the asymmetry is not only a property determined by the

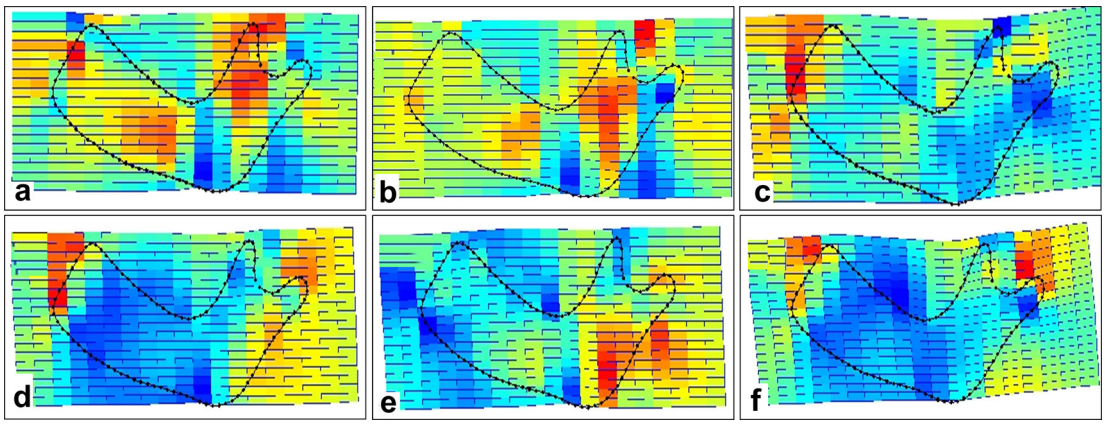

Figure 6 Variation of the shape in females.

size, but also the mandibular right curve is significantly dissimilar to the mandibular left curve. Taking this in to account to achieve a real mandibular prediction, asymmetry is a factor that must be considered in further studies.

On the other side, it is well-known that tomography images are precise and with them volume analysis, surface size, curvature, bone mineral density (BMD), among others, can be performed.[12] Nevertheless, for the main purpose of the present study, EFA allowed to statistically reach a deeper search of differences in shape morphology that cannot be accomplished in some studies that used only linear and angular measurements, even if they are using CT scans.[6,18] Such results are found not only in sexual difference, in general or specific asymmetry, but also in the differentiation of skeletal patterns.

In Figures 4 and 5 can be seen the general distribution of skeletal classes, which is from the bottom to top, Class II, Class I and Class III in all groups. This is consistent because the ANB angle is a spectrum of continuous measures that discriminates the general facial form with one degree of difference between its limits. Unlike previous studies on the same research line,[14] in this case the differentiation of Class II and Class I was evident except in Class I males' right side. This means that the exploration in the shape of the classes or even different groupings other than Steiner's classifications is necessary because it could determine a practical differentiation which would also help with the processes of prediction of the mandibular morphology.

Additionally, it can be observed that the shape of Class III can easily be distinguished from the other two; however these differences are not noticeable from the shape according to the heat maps, where more extensive regions in red color could be expected along the general morphology. The variation was found only specific sites, maybe demonstrating a great influence of this class of the general consensus and for this reason there is not any major differences. This could explain the reason of the greater differences of Class II male right side with respect to the general consensus in most of its morphology in the heat maps (Figure 7e); this information is also reflected in Figure 5 because this group (0M2) is widely separated from Class I and III.

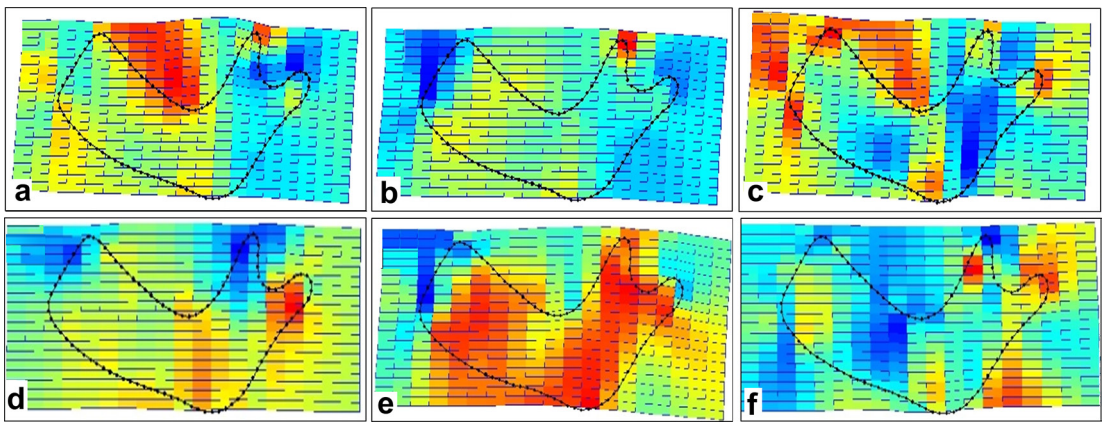

Figure 7 Variation of the shape in males.

Finally, our findings support the hypothesis that despite the morphological differences among the skeletal classes, none of them display a particular trend toward left-right asymmetry. This is because a relation between side and class was not found as seen in Tables 4 and 5. Although the results showed relevance to determine that the shape asymmetry is natural in patients, it can only be extrapolated only to the central region of the Colombian population, which makes it necessary to do an exploration of other populations that will allow generalizing the results. This will ensure the improvement of the algorithms for the prediction systems for a more accurate mandibular reconstruction.

In conclusion, there is a general asymmetry and asymmetry by sex, hence shape asymmetry is natural in all the studied patients; however despite also finding differences between classes, asymmetry is not a characteristic of only one class and cannot be related only to pathological processes; besides, it is important to consider these findings to enhance the current reconstruction systems or create an automated model of mandibular prediction with these output variables.

Acknowledgement

The authors are grateful to the Brazilian fostering agency Coordenação de Aperfeiçoamento de Pessoal de Nível Superior (CAPES), Conselho Nacional de Desenvolvimento Científico e Tecnológico (CNPq), and the partnerships Program for Education and Training (PAEC), Organization of American States (OAS), and the Coimbra Group of Brazilian Universities (GCUB) (PAEC OEA-GCUB 2015 Scholarship).

References

1. Solem RC, Ruellas A, Miller A, Kelly K, Ricks-Oddie JL, Cevidanes L, et al. Congenital and acquired mandibular asymmetry: mapping growth and remodeling in 3 dimensions. *Am J Orthod Dentofacial Orthop* 2016; **150**: 238–51. doi: https://doi.org/10.1016/j.ajodo.2016.02.015
2. Leamy L, Klingenberg C, Sherratt E, Wolf J, Cheverud J. The genetic architecture of fluctuating asymmetry of mandible size and shape in a population of mice: another look. *Symmetry* 2015; **7**: 146–63. doi: https://doi.org/10.3390/sym7010146
3. Thiesen G, Gribel BF, Freitas MP. Facial asymmetry: a current review. *Dental Press J Orthod* 2015; **20**: 110–25. doi: https://doi.org/10.1590/2177-6709.20.6.110-125.sar
4. Chen YJ, Yao CC, Chang ZC, Lai HH, Lu SC, Kok SH. A new classification of mandibular asymmetry and evaluation of surgical-orthodontic treatment outcomes in Class III malocclusion. *J Craniomaxillofac Surg* 2016; **44**: 676–83. doi: https://doi.org/10.1016/j.jcms.2016.03.011
5. Thiesen G, Gribel BF, Kim KB, Freitas MPM. Maxillofacial features related to mandibular asymmetries in skeletal Class III patients. *J Oral Maxillofac Surg* 2017; **75**: 1015–25. doi: https://doi.org/10.1016/j.joms.2016.11.011
6. Sanders DA, Chandhoke TK, Uribe FA, Rigali PH, Nanda R. Quantification of skeletal asymmetries in normal adolescents: cone-beam computed tomography analysis. *Prog Orthod* 2014; **15**: 26. doi: https://doi.org/10.1186/s40510-014-0026-0
7. Kheir NA, Kau CH. Measuring mandibular asymmetry in Class I normal subjects using 3D novel coordinate system. *Ann Maxillofac Surg* 2014; **4**: 34. doi: https://doi.org/10.4103/2231-0746.133073
8. Niño Sandoval TC, Guevara Pérez SV, González FA, Jaque RA, Infante Contreras C. Uso de redes neuronales artificiales en predicción de morfología mandibular a través de variables craneomaxilares en una vista posteroanterior. *Univ Odontol* 2016; **35**: 21–8.
9. Chen SY, Lestrel PE, Kerr WJ, McColl JH. Describing shape changes in the human mandible using elliptical Fourier functions. *Eur J Orthod* 2000; **22**: 205–16. doi: https://doi.org/10.1093/ejo/22.3.205
10. Schmittbuhl M, Le Minor JM, Schaaf A, Mangin P. The human mandible in lateral view: elliptical fourier descriptors of the outline and their morphological analysis. *Ann Anat* 2002; **184**: 199–207. doi: https://doi.org/10.1016/S0940-9602(02)80021-8
11. Lestrel PE, Wolfe CA, Bodt A. Mandibular shape analysis in fossil hominins: fourier descriptors in norma lateralis. *Homo* 2013; **64**: 247–72. doi: https://doi.org/10.1016/j.jchb.2013.05.001
12. Lin H, Zhu P, Lin Y, Wan S, Shu X, Xu Y, et al. Mandibular asymmetry: a three-dimensional quantification of bilateral condyles. *Head Face Med* 2013; **429**: 42. doi: https://doi.org/10.1186/1746-160X-9-42
13. Alhadidi A, Cevidanes LH, Paniagua B, Cook R, Festy F, Tyndall D. 3D quantification of mandibular asymmetry using the SPHARM-PDM tool box. *Int J Comput Assist Radiol Surg* 2012; **7**: 265–71. doi: https://doi.org/10.1007/s11548-011-0665-2
14. Niño-Sandoval TC, Guevara Perez SV, González FA, Jaque RA, Infante-Contreras C. An automatic method for skeletal patterns classification using craniomaxillary variables on a Colombian population. *Forensic Sci Int* 2016; **261**: 159.e1–159.e6. doi: https://doi.org/10.1016/j.forsciint.2015.12.025
15. Ministerio de Salud. *Resolución 8430 de 1993. Minist Salud y Protección Soc República Colomb*. **1993**; 1993. pp. 1–19.
16. Montenegro J V, González Vasques E, Contasti G. Influencia de la Mordida Cruzada posterior Unilateral en el crecimiento mandibular. *Rev Latinoam Ortod y Odontopediatría* 2006; **1**: 1–10.
17. Khalifa GA, Abd El Moniem NA, Elsayed SA, Qadry Y. Segmental mirroring: does it eliminate the need for intraoperative readjustment of the virtually pre-bent reconstruction plates and is it economically valuable? *J Oral Maxillofac Surg* 2016; **74**: 621–30. doi: https://doi.org/10.1016/j.joms.2015.09.036
18. Inoue K, Nakano H, Sumida T, Yamada T, Otawa N, Fukuda N, et al. A novel measurement method for the morphology of the mandibular ramus using homologous modelling. *Dentomaxillofac Radiol* 2015; **44**: 20150062. doi: https://doi.org/10.1259/dmfr.20150062